

Accounting all contributions for the Van Vleck paramagnetism and the Langevin diamagnetism from first principles: application to diamond

A. V. Nikolaev,¹ I. I. Vlasov,² and L. L. Tao³

¹Skobeltsyn Institute of Nuclear Physics, Moscow State University, Vorob'evy Gory 1/2, 119234, Moscow, Russia

²Prokhorov General Physics Institute of the Russian Academy of Sciences, 119991 Moscow, Russia

³School of Physics, Harbin Institute of Technology, Harbin 150001, China

A general method for calculating magnetic susceptibility (χ) in dielectrics within a single choice of magnetic gauge for the whole crystal is presented. On the basis of the method, accounting for all contributions to the Van Vleck paramagnetism and Langevin (Larmore) diamagnetism, a full-scale *ab initio* calculation of χ in diamond is performed. Unfamiliar contributions to χ includes a Van Vleck contribution from the interstitial region and an offset contribution from the muffin-tin (MT) sphere, appearing due to the change of the MT-sphere magnetic moment when the sphere is displaced from the origin. Although the Langevin diamagnetism explicitly depends on the choice of the origin, its sum with the Van Vleck term remains invariant, which is demonstrated on the basis of the gauge invariance of the magnetic vector potential. The derived expressions have been applied to *ab initio* calculations of magnetic susceptibility of the crystalline diamond within the linear augmented plane wave method (LAPW). With the diamond unit cell having the inversion symmetry, the magnetic (Van Vleck) calculations require the irreducible part of the Brillouin zone accounting for half of the whole zone, i.e. 24 times larger than that in the absence of magnetic field. Investigating possible anisotropy of χ , we calculate it for 74 different directions of H (belonging to Lebedev surface grid points), and demonstrate that the actual value of χ remain isotropic. The obtained volume magnetic susceptibility in diamond lies in the range $-16.27 - 16.72$ (with the Langevin contribution $-39.22 - 39.94$ and the Van Vleck contribution $-22.94 - 23.22$), in units 10^{-7} , which compares well with the experimental data and other calculations.

I. INTRODUCTION

The task of predicting magnetic properties of solids and nano-structures is of fundamental importance. If, thanks to the rapid development of *ab initio* calculations, which are now regularly used in experimental and theoretical studies, the problem of obtaining and predicting the electronic structure can be considered generally solved, then the situation with magnetic properties is still far from this stage. On the other hand, the progress in practical magnetic applications is closely related to spintronics, which manipulates very sensitive electronic or nuclear spin degrees of freedom [1]. In particular, much attention recently has been drawn by new research in detection, characterization and manipulation by nitrogen-vacancy (NV^-) centers [2, 3] and ^{13}C nuclear spins in diamond [4–6]. The problem is of great practical importance – it is believed that the emerging techniques can be used in magnetometer of extreme sensitivity [2, 7] and nano-scale resolution [8–10]. Other applications include bioimaging under ambient conditions [8, 11] and quantum information processing [9, 12, 13]. Since correlated ^{13}C nuclear spin states can be very long-lived [14], nuclear spin hyperpolarization generated from NV-vacancy centres in diamond is considered as a possible platform for polarization transfer to samples for nuclear magnetic resonance spectroscopy and magnetic resonance imaging [4–6, 15–18]. To understand the mechanism and advance the NV- and ^{13}C based technologies, knowledge of the host material magnetic properties (both diamagnetic and paramagnetic) is undoubtedly necessary. There are very few experimental works on magnetic behavior of diamond

[19, 20] in the literature, which is undoubtedly related to the technical complexity of such measurements [21]. Therefore, the study of the magnetic response of diamond at *ab initio* level, which is free from assumptions and suggestions, is of primary interest.

Early attempts to calculate the magnetic susceptibility of diamond and other insulators were based on partially semiempirical models [19, 22–24]. The first method for the calculation of the magnetic susceptibility of insulators from first principles was developed in 1996 in the pioneer work of Mauri and Louie [25]. The external magnetic field H in this work was modulated with a finite wave vector $\vec{q} \neq 0$, and the diamagnetic part (proportional to $A^2 \propto q^{-2}$, where A is the vector potential) by means of the *f*-sum rule was rewritten through a sum $g(\vec{k}, \vec{k})$, which was also used for the calculation of the paramagnetic part ($\propto \vec{p} \vec{A}$). Thus, both contributions are expressed in terms of the same function $g(\vec{k}, \vec{k}')$, which in practice removes the numerical instability associated with the q^{-2} dependence in χ . The full response was calculated taking the limit at $\vec{q} \rightarrow 0$, i.e. at the infinite wavelength of the modulation. The *f*-sum rule implies a certain choice of gauge. In [26] it is shown that for finite systems the Mauri, Pfrommer, and Louie (MPL) method [27], which extends the concept of [25] to the problem of chemical shift calculations, is equivalent to the continuous ($d(r) = r$) set of gauge transformation (CSGT). In the following the focus of the research was shifted to *ab initio* calculations of nuclear magnetic resonance (NMR) chemical shifts on the basis of the MPL approach [27]. The early version of the method [25, 27] was limited to light elements with hard pseudopotentials. In later de-

velopment these limitations have been overcome in subsequent works [28] and [29].

Following the approach of [28, 29], the formalism was developed and implemented for a full potential all electron augmented plane wave (APW) method used for precise calculations of electron band structure [30, 31]. In this method there are no restrictions imposed on the electron density or induced electron current, and the integration is performed without further approximations. Nevertheless, the formalism still requires the modulation with the wave vector \vec{q} of either the magnetic field [25, 27] or the position operator [28], and as before the actual results are obtained in the limit $q \rightarrow 0$. As [25, 27] the method employs the continuous ($d(r) = r$) gauge for the valence electrons. Although the studies [30, 31] aim mainly the NMR chemical shifts, the magnetic susceptibility can also be calculated. The obtained values of χ for some fluorides, oxides, chlorides and bromides are quoted in Table I of Ref. [31].

In the present study we work within a single choice of the gauge for the vector potential \vec{A} , Eq. (2), with its origin, \vec{R}_0 , situated at the center of the first primitive unit cell ($n = 1$), Fig. 1, located at the origin of the coordinate system. This, in particular, implies, that the vector potential \vec{A} is different in all other unit cells ($n \neq 1$). However, as discussed in Sec. II and Appendix A below, the contributions from other cells will be the same due to the gauge invariance. Our approach differs from the continuous gauge ($d(r) = r$) used in other treatments [25, 27, 30, 31]. We also do not use the modulation of the external magnetic field with the wave vector q , working in the fully static environment, $q \equiv 0$. Our method for the Van Vleck and Langevin contributions [32] is directly applicable to any solid, not only to dielectrics, but also to metals. Of course, in the case of metals, the Pauli paramagnetism and the Landau diamagnetism should be taken into account as well [33, 34].

Our main goal here is to study possible anisotropy of χ in cubic diamond. It is worth noting that the magnetic anisotropy does present in cubic crystals – e.g. the well known textbook example of magnetocrystalline anisotropy in ferromagnetic cubic structures of iron and nickel [35]. On the other hand, theoretically it is shown that there is an explicit dependence of χ on the direction of \vec{H} for cubic alkali metals due to the Landau diamagnetism [36]. Therefore, *a priori* we can not state that in the case of diamond there is no such an anisotropy.

In diamond and other dielectrics the magnetic susceptibility is limited only by Van Vleck and Langevin contributions. Although these two terms are known for many decades, in the next section we will see that within the single choice of gauge for the whole crystal, adopted in the present study, they can take unfamiliar forms, such as those originating from the interstitial region (Sec. III C below) or resulting in offset terms related to the displacement of MT-spheres (Sec. III B and Eq. (14) below). Finally, we note that all our numerical calculations are based on *ab initio* band structure calculations of di-

amond, using the full potential linear augmented plane wave method (FLAPW) [37, 38] as implemented in Ref. [39], with technical parameters given in Sec. III A.

The paper is organized as follows. In Sec. II we discuss the origin of additional terms in our single gauge approach, in Sec. III and Sec. IV we derive explicit expressions for the Van Vleck paramagnetic and Langevin diamagnetic contributions. In Sec. V the method is applied to the diamond, where we calculate χ for various directions of \vec{H} and conclude that χ is isotropic. Our conclusions are summarized in Sec. VI.

II. METHOD: EXTRA CONTRIBUTIONS TO χ IN THE SINGLE GAUGE APPROACH

As mentioned in the introduction, we work with a single choice of magnetic gauge throughout the whole crystal. In the final expressions given in Sec. III and Sec. IV for valence electrons the gauge origin \vec{R}_0 [see Eq. (2)] coincides with the origin of the coordinate system, i.e. $\vec{R}_0 = 0$, and the focus is on the first ($n = 1$) unit cell, Fig. 1. However, in this section for methodological purposes we also consider the case $\vec{R}_0 \neq 0$, and discuss the most important consequences of our approach: the dependence of partial contributions on the choice of the gauge origin, and the appearance of additional contributions to χ . Since we aim to study possible anisotropy of χ , in all equations below we stress out the dependence on the direction of H .

In general, there are two different mechanisms for diamagnetism: the Landau diamagnetism of itinerant electrons [34] and the Langevin diamagnetism [32] (equivalent to the Larmor precession in the presence of the center of attraction). In dielectrics or semiconductors the electron spectrum exhibits a gap at the Fermi level, separating the valence and conduction band. The density of states at the Fermi level (or chemical potential) $N(E_F) = 0$, which implies that the Pauli paramagnetism is excluded, $\chi_{Pauli} = 0$. In such a case, the Landau diamagnetism is also absent, because a fully occupied electron band results in zero contribution, $\chi_{Landau} = 0$ [36].

Thus, the diamagnetism in our case can be exclusively of the Langevin (χ^{dia}) type and the paramagnetism of the Van Vleck (χ^{para}) type. The Langevin diamagnetism χ^{dia} includes the core and valence electron contributions (χ_c^{dia} and χ_{val}^{dia}) given by [34, 40]

$$\chi^{dia} = -\frac{e^2}{4mc^2} \langle r_{\perp}^2 \rangle, \quad (1)$$

where $\langle r_{\perp}^2 \rangle$ stands for averaging over the core electron density $\rho_{core}(r)$ or valence electron density $\rho_{val}(r)$. Here r_{\perp} stands for the component of the radius vector \vec{r} , perpendicular to the direction of the magnetic field H , $\vec{n}_H = \vec{H}/H$. Equivalently, the component \vec{r}_{\perp} is perpen-

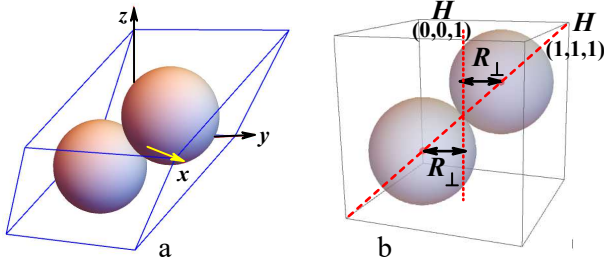


FIG. 1. (a) The diamond unit cell with two touching MT-spheres with the centers at $\vec{R}_c = \pm(1, 1, 1)a/8$. The origin $O(0, 0, 0)$ is at the center of the unit cell, which is also the inversion center. (b) Perpendicular components R_{\perp} of the MT-sphere centers \vec{R}_c in respect to two lines of zero vector potential \vec{A} (for $\vec{H} \parallel (1, 1, 1)$ and $\vec{H} \parallel (0, 0, 1)$)

dicular to the zero line of the vector potential \vec{A} , because

$$\vec{A} = \frac{1}{2} \vec{H} \times (\vec{r} - \vec{R}_0) = \frac{1}{2} r_{\perp} H \vec{e}_{\perp, H} \quad (2)$$

is perpendicular to \vec{r}_{\perp} and to the direction of \vec{n}_H , with the unit vector $\vec{e}_{\perp, H} \sim \vec{r}_{\perp} \times \vec{n}_H$. The vector \vec{R}_0 corresponds to the gauge origin. We start with $\vec{R}_0 = 0$, but later consider cases with $\vec{R}_0 \neq 0$. For the averaged value, $\langle r_{\perp}^2 \rangle$, we have,

$$\langle r_{\perp}^2 \rangle = \int_V \rho(r) r_{\perp}^2 dv, \quad (3)$$

where the integration is taken over the unit cell region (with the volume V). In the case of core electron shells the electron density ρ_c is spherical and confined by the interior region of MT-spheres centered at nuclei. In that case the region of integration in Eq. (3) is simply the MT-spheres, shown for the diamond unit cell in Fig. 1. For the valence electrons (ρ_{val}), the integration should be performed over the whole unit cell including the interstitial region.

The important feature of the Langevin diamagnetism χ^{dia} is that it explicitly depends on the choice of the gauge origin through \vec{R}_0 in Eq. (2). Suppose that we find $\chi_{MT,0}^{dia} = -C_L \langle r_{\perp}^2 \rangle_c$ (here $C_L = e^2/4mc^2$) for the electrons confined strictly inside a MT sphere, whose center \vec{R}_c coincides with the origin (i.e. $\vec{R}_c = \vec{R}_0 = 0$). If now we calculate $\chi_{MT,R}^{dia}$ for the MT-sphere displaced from $O(0, 0, 0)$ through the translation by the vector \vec{R} , we obtain

$$\begin{aligned} \chi_{MT,R}^{dia} &= -C_L \langle (\vec{r} + \vec{R})_{\perp}^2 \rangle_c \\ &= \chi_{MT,0}^{dia} - C_L R_{\perp}^2 |Q^{MT}|, \end{aligned} \quad (4)$$

where R_{\perp} is the component of \vec{R} perpendicular to \vec{H} , and Q^{MT} is the total electron charge inside the MT-sphere. In Eq. (4) we have assumed that the dipole momentum of the whole sphere, counted from its center, is zero, i.e. $\langle r_{\perp} \rangle_c = 0$. Note, that $\langle r_{\perp} \rangle_c \neq 0$ can occur

in ferroelectrics; in most cases, including diamond, it is absent. R_{\perp} for two spheres in the diamond unit cell explicitly depends on the direction of H . For example, as shown in Fig. 1b for the field direction $[1, 1, 1]$ $R_{\perp} = 0$, whereas for $[0, 0, 1]$ $R_{\perp} \neq 0$. From Eq. (4) it follows that $|\chi_{MT,R}^{dia}| > |\chi_{MT,0}^{dia}|$.

The total susceptibility, $\chi^{tot} = \chi^{dia} + \chi^{para}$, however, includes also the paramagnetic Van Vleck term [40],

$$\chi^{para} = 2 \sum_{i' \neq i} \frac{|(M_H)_{i'i}|^2}{E_j^{(0)} - E_i^{(0)}}. \quad (5)$$

The sum of two terms, $\chi^{dia} + \chi^{para}$, does not depend on the choice of the gauge origin [\vec{R}_0 in Eq. (2)] and the translation vector \vec{R} discussed above. $(M_H)_{i'i}$ in Eq. (5) is the matrix element of the \vec{n}_H -component of the magnetic moment \vec{M} (i.e. in the direction of the magnetic field H), $E_j^{(0)}$ is the energy spectrum, the ground state is described by $|i = 1\rangle$ and the summation in Eq. (5) is taken over all excited states $i' = 2, 3, \dots$. Similarly to the Langevin part, χ^{para} depends on the choice of \vec{R}_0 , because upon the translation through \vec{R} for the matrix elements $(M_H)_{i'i} = \mu_B (L_H)_{i'i}$ we obtain

$$\begin{aligned} \langle M'_H \rangle &= \mu_B \langle (\vec{r} + \vec{R}) \times \vec{p} \rangle \cdot \vec{n}_H \\ &= \langle M_H \rangle + \mu_B \vec{R}_{\perp} \times \langle \vec{p}_{\perp} \rangle \cdot \vec{n}_H, \end{aligned} \quad (6)$$

(The spin contribution to M_H is zero, see Sec. III and Eq. (8) below.) In Eq. (6) $\langle M'_H \rangle$ is the matrix elements in the new coordinate system, $\vec{p} \equiv -i\vec{\nabla}$ is the operator of momentum (in atomic units) and $\langle \dots \rangle \equiv \langle i' | \dots | i \rangle$. In Eq. (6) only the perpendicular components of \vec{R} and \vec{p} are involved. Thus, in diamond for $\vec{H} \parallel z$ with $R_{\perp} \neq 0$, Fig. 1b, the calculation of the magnetic moments $\langle M_H \rangle$ inside a displaced MT-sphere requires the matrix elements $\langle i | p_{\nu} | i' \rangle$ of momentum ($\nu = x, y$). It is not obvious that the change in χ^{dia} e.g. in Eq. (4) is exactly compensated by the change of χ^{para} through the transformation of $\langle M'_H \rangle$, given in Eq. (6), especially taking into account that the Langevin contribution is solely due to the electron density (i.e. the ground state quantity) while the Van Vleck term explicitly involves the excited quantum states i' in $\langle M'_H \rangle$. First prove of that was sketched by Van Vleck in Ref. 32, where the change of χ^{tot} was considered through laborious algebraic transformation in the energy representation for an infinitesimal increment of δx . In Appendix A we present a compact prove of it in general form on the basis of the gauge invariance of the vector potential \vec{A} . In fact, the statement of Appendix A is a cornerstone of all present consideration, because it ensures that the contribution to χ from any unit cell n of the crystal is exactly the same as from the unit cell $n = 1$ situated at the origin, Fig. 1, even though we work within a single choice of gauge for the whole crystal.

Additional magnetic contributions (“offset terms”) are given by second terms on the right hand sides of Eq. (4) and Eq. (6).

In principle, the approach outlined here should be equally applied to the valence and core electron states. In practice, however, it seems reasonable to use it only for the valence electrons. The main problem is numerous offset contributions from the magnetic moment due to the nonzero matrix elements of momentum $\langle \vec{p}_\perp \rangle$ in the right hand side of Eq. (6). For example, considering the $1s$ core states of carbon, we obtain nonzero matrix elements of the type $\langle i' | \vec{p}_\perp | 1s \rangle$, where i' is np excited electron states ($n = 2, 3, \dots$). In the case of core states, it is possible to avoid dealing with these contributions by working with the gauge origin, coinciding with the MT-sphere center where $\vec{R}_\perp = 0$. (For the valence states of diamond and other solids with few atoms in the unit cell this is not possible [24].) With this choice of gauge, there is no contribution from the Van Vleck term, because for the $1s$ states $\langle M_H \rangle = 0$, and one has to evaluate only the diamagnetic term. According to the gauge invariance of the sum $(\chi_c^{dia} + \chi_c^{para})$, Appendix A, the same core contribution is obtained with any other gauge origin \vec{R}_0 . Thus, the core contribution for carbon is calculated easily. However, in general the core configuration can also contain p - and d -atomic states, split by an appreciable spin-orbit coupling, which makes the precise evaluation difficult. For example, the silicon core configuration is $1s^2 2s^2 2p^6$, and the magnetic moment matrix elements $\langle i' | M_H | 2p \rangle$ differ from zero for $i' \equiv np$ excited states ($n = 3, 4, \dots$). For silicon therefore, the Van Vleck contribution is not zero and there appears a problem of full representation of excited states. All these effects are beyond the scope of the present consideration and will be described elsewhere.

III. METHOD: VAN VLECK PARAMAGNETISM

The Van Vleck paramagnetic contribution χ^{para} to the magnetic susceptibility χ^{tot} , adapted for the band structure case, can be written in the following form [24]:

$$\chi^{para} = 2 \sum_{\vec{k}} w(\vec{k}) \sum_a^{N_b^o} \sum_p^{N_b^{uno}} \frac{|\langle p | M_H(\vec{k}) | a \rangle|^2}{E_p(\vec{k}) - E_a(\vec{k})}. \quad (7)$$

Here, the first summation (on a) is taken over all occupied bands N_b^o and the second (on p) over unoccupied bands N_b^{uno} . In general, in Eq. (7) one has to integrate over all points \vec{k} belonging to the first Brillouin zone. In practice the summation is taken over a set of a representative k -points, Sec. III A, with corresponding k -weights $w(k)$. For diamond the Fermi level (or rather, the chemical potential μ) lies in the energy gap between $a = 4$ and $p = 5$ band states. Therefore, in Eq. (7) the sum on a is performed over four lowest occupied bands, i.e. $N_b^o = 4$ and $a = 1 - 4$, while for the sum over unoccupied bands we have $p \geq 5$. The upper limit for the unoccupied bands, N_b^{uno} , is determined by the

dimension N_b of the basis set used for the band structure calculation, $N_b^{uno} = N_b - N_b^o$. (In most of our diamond calculations $N_b^{uno} = 259$.)

The electron magnetic operator is given by $M_H \equiv M_{z'} = \mu_B(g_s s_{z'} + L_{z'})$, where μ_B is the Bohr magneton and $g_s \approx 2$ is the electron g -factor. Here the z' -axis correspond to the direction \vec{n}_H of the external magnetic field \vec{H} introduced earlier. Note that in the absence of the spin-orbit coupling, due to the orthogonality of the band states at each k -point, we have $\langle p | a \rangle = 0$ ($a \neq p$) and hence $\langle p | s_{z'} | a \rangle = 0$. Therefore, the contribution to χ^{para} stems only from the matrix elements of the orbital momentum $L_H \equiv L_{z'}$, and

$$\langle p | M_H(\vec{k}) | a \rangle = \mu_B \langle p | L_H(\vec{k}) | a \rangle. \quad (8)$$

In practice we obtain the eigenstates $|a\rangle$, $|p\rangle$ from electron band structure calculations. In LAPW for example, one solves the eigenstate problem in the basis of augmented plane waves ϕ_j [see Eq. (10) below], and, as a result, obtains the eigenstates as the coefficients of expansion in the basis set, i.e. $\langle j | a \rangle$ and $\langle j | p \rangle$. The quantity $\langle p | L_H(\vec{k}) | a \rangle$ then is obtained through the matrix transformation from $\langle t | L_H(\vec{k}) | j \rangle$, defined in the basis of $|j\rangle$. Therefore, the main task becomes to calculate the matrix elements of $\langle t | L_H(\vec{k}) | j \rangle$ in terms of basis functions ϕ_j . Below, we consider all different contributions to $\langle t | L_H(\vec{k}) | j \rangle$, comprising L_H^{MT} , coming from MT-spheres, and L_H^{IR} from the interstitial region. Further, $L_H^{MT} = L_H^{MT,I} + L_H^{MT,II}$, where $L_H^{MT,II}$ is the offset term, Sec. III B. Matrix elements of full magnetic moment M_H in terms of ϕ_j are thus given by

$$\begin{aligned} \langle t | M_H(\vec{k}) | j \rangle = & \mu_B (\langle t | L_H^{MT,I}(\vec{k}) | j \rangle + \langle t | L_H^{MT,II}(\vec{k}) | j \rangle \\ & + \langle t | L_H^{IR}(\vec{k}) | j \rangle). \end{aligned} \quad (9)$$

A. LAPW basis functions and computation details

The LAPW method [37, 38] is probably the most precise all-electron method for band structure calculations, widely used for studies of bulk materials.

In the LAPW method space is partitioned in the region inside the nonoverlapping MT-spheres and the interstitial region IR . The basis functions $\phi_j(\vec{k}, \vec{R})$, where $j = 1, 2, \dots, N_b$, are given by

$$\phi_j(\vec{k}, \vec{R}) = \begin{cases} V^{-1/2} \exp(i(\vec{k} + \vec{K}_j)\vec{R}), & \vec{R} \in IR \\ \sum_{l,m} \mathcal{R}_{l,m}^{j,\alpha}(r, E_l) Y_{l,m}(\hat{r}), & \vec{R} \in MT(\alpha) \end{cases} \quad (10)$$

where \vec{K}_j refers to the reciprocal lattice vector j , $Y_{l,m}$ are spherical harmonics [41] and the radial part is given by

$$\mathcal{R}_{l,m}^{j,\alpha}(r, E_l) = A_{l,m}^{j,\alpha} u_l(r, E_l) + B_{l,m}^{j,\alpha} \dot{u}_l(r, E_l).$$

Here the index α refers to the type of atom (or MT-sphere) in the unit cell, the radius r is counted from the

center \vec{R}_α of the sphere α (i.e. $\vec{r} = \vec{R} - \vec{R}_\alpha$), V is the volume of the unit cell. Radial functions $u_l(r, E_l)$ are solutions of the Schrödinger equation in the spherically averaged crystal potential computed at the linearization energy E_l , and $\dot{u}_l(r, E_l)$ is the derivative of u_l with respect to E at E_l . The coefficients $A_{l,m}^{j,\alpha}$ and $B_{l,m}^{j,\alpha}$ are found from the condition that the basis function ϕ_j is continuous with continuous derivative at the sphere boundary, $r = R_{MT}^\alpha$ (R_{MT}^α is the radius of the MT-sphere α):

$$A_{l,m}^{j,\alpha} = \frac{4\pi}{\sqrt{V}} i^l R_{MT}^2 Y_{l,m}^*(\hat{k}_j) e^{i\vec{k}_j \vec{R}_\alpha} a_l^j,$$

$$B_{l,m}^{j,\alpha} = \frac{4\pi}{\sqrt{V}} i^l R_{MT}^2 Y_{l,m}^*(\hat{k}_j) e^{i\vec{k}_j \vec{R}_\alpha} b_l^j.$$

Here $\vec{k}_j = \vec{k} + \vec{K}_j$ and we have introduced the standard LAPW quantities a_l^j , b_l^j , expressed only through the spherical Bessel functions j_l and the radial solution u_l (and its derivatives) at $r = R_{MT}^\alpha$.

For diamond there are two carbon MT-spheres in the unit cell related through the inversion symmetry, Fig. 1. Computation of χ^{dia} , χ^{para} and χ^{tot} were performed with the core and valence electron densities obtained as a result of the self-consistent procedure within the FLAPW band structure method [37, 38], implemented in Ref. [39]. Diamond is crystallized in the diamond structure consisting of two simple face-centered cubic (fcc) Bravais lattices [33, 35], with two equivalent atoms in the primitive unit cell, Fig. 1. In Fig. 1 the edges of the unit cell are collinear to three basis vectors \vec{b}_ν ($\nu = 1, 2, 3$) defined as in Ref. [41]: $\vec{b}_1 = (0, 1, 1) a/2$, etc. The technical parameters of numerical calculations for diamond are the same as those used in Ref. [24]. The number of augmented plane waves was 259-283 with the wave vectors \vec{K}_j satisfying the condition $R_{MT} K_j \leq 8.25$. The maximal number of k -points in the irreducible part of the first Brillouin zone (BZ) was 2304, and the maximal value of the LAPW plane-wave expansion was $l_{max} = 8$. We have used the tetrahedron method for the linear interpolation of energy between k points [42]. For calculation of the exchange-correlation potential and the exchange-correlation energy contribution within the DFT approach, we have used the Perdew-Burke-Ernzerhof (PBE) variant [43] of the generalized-gradient approximation (GGA) and the variant of the local density approximation (LDA) with the standard ($V_{exc} \sim -\rho^{1/3}$) exchange [44] and the PW-correlation [45]. The number of radial points inside the MT region was increased to 1000. Finally, there were 21822 points used in the interstitial region of the unit cell. Test calculations of the equilibrium lattice constants a_{latt} and bulk moduli B for diamond confirm the results of [24]: $a_{latt}^{LDA} = 3.549$ Å, $B^{LDA} = 474.8$ GPa (LDA) and $a_{latt}^{GGA} = 3.592$ Å, $B^{GGA} = 440.1$ GPa (GGA), and are in good correspondence with experimental data (3.567 Å and 442 GPa). Calculations of the magnetic susceptibility have been performed for three different lattice constants, a_{latt}^{LDA} , a_{latt}^{GGA} , and the experimental lattice constant a_{latt}^{exp} .

B. Magnetic Moment inside MT-spheres

The expression for the matrix elements of the orbital momentum $L_H^{MT,I}(\vec{k}, \alpha)$ and the corresponding magnetic moment $M_H^{MT,I} = \mu_B L_H^{MT,I}$ inside the MT-sphere α along \vec{n}_H , defined in respect to the MT-sphere center \vec{R}_α , can be obtained e.g. from equations quoted in Ref. [46]:

$$\langle t | L_H^{MT,I}(\vec{k}, \alpha) | j \rangle = \langle t | \vec{L}^I(\vec{k}, \alpha) | j \rangle \vec{n}_H, \quad (12a)$$

$$\langle t | \vec{L}^{MT,I}(\vec{k}, \alpha) | j \rangle = -i \frac{4\pi R_\alpha^4}{V} e^{i\vec{K}_{tj} \vec{R}_\alpha} \mathcal{S} \vec{\mathcal{K}}, \quad (12b)$$

where $\vec{\mathcal{K}} = [\hat{k}_t \times \hat{k}_j]_{x,y,z}$, $\hat{k} = \vec{k}/k$, $\vec{K}_{tj} = \vec{K}_j - \vec{K}_t$ and

$$\mathcal{S} = \sum_l (2l+1) P'_l(\hat{k}_t \hat{k}_j) (a_l(\vec{k}_t) a_l(\vec{k}_j) + b_l(\vec{k}_t) b_l(\vec{k}_j) N_l). \quad (12c)$$

Here $P'_l(x)$ is the derivative of the Legendre polynomial, and $N_l = \langle \dot{u}_l | \dot{u}_l \rangle$ is the radial integral of $\dot{u}_l^2(r)$ inside the MT-sphere α [46].

However, as discussed in Sec. II, in reality the orbital momentum has to be evaluated in respect to another point – the gauge origin \vec{R}_0 , which does not necessarily coincide with the MT-sphere center \vec{R}_α . In particular, this has to be done for any unit cell with few MT-spheres, for example, for the diamond unit cell in Fig. 1b. In that case, as follows from Eq. (6), we should account for the extra magnetic term $\mu_B \vec{R} \times \langle \vec{p} \rangle \cdot \vec{n}_H$, where $\langle \vec{p} \rangle$ stands for the matrix elements of the momentum inside the MT-sphere α , i.e.

$$L_H^{MT}(\vec{k}, \alpha) = L_H^{MT,I}(\vec{k}, \alpha) + L_H^{MT,II}(\vec{k}, \alpha). \quad (13)$$

Here the contribution $L_H^{MT,II}(\vec{k}, \alpha)$ is associated with the offset of the MT-sphere from the line of zero vector potential \vec{A} . Matrix elements of $L_H^{MT,II}(\vec{k}, \alpha)$ are written as

$$\langle t | L_H^{MT,II}(\vec{k}, \alpha) | j \rangle = \left[\vec{n}_H \times \vec{R}_\alpha e^{i\vec{K}_{tj} \vec{R}_\alpha} \right] \langle t | \vec{P}(\vec{k}, \alpha) | j \rangle \quad (14)$$

where $\langle \vec{P}(\vec{k}, \alpha) \rangle$ is the matrix element of momentum inside the MT-sphere α ,

$$\langle t | \vec{P}(\vec{k}, \alpha) | j \rangle = C_\alpha \sum_{l_j, \tau_j} \sum_{l_t, \tau_t} i^{l_j - l_t - 1} Y_{l_t, \tau_t}(\hat{k}_p) Y_{l_j, \tau_j}^*(\hat{k}_j) \{ a_{l_t} a_{l_j} (u Y_{l_t, \tau_p} | \vec{\nabla} u Y_{l_j, \tau_j}) + a_{l_t} b_{l_j} (u Y_{l_t, \tau_p} | \vec{\nabla} \dot{u} Y_{l_j, \tau_j}) + b_{l_t} a_{l_j} (\dot{u} Y_{l_t, \tau_p} | \vec{\nabla} u Y_{l_j, \tau_j}) + b_{l_t} b_{l_j} (\dot{u} Y_{l_t, \tau_p} | \vec{\nabla} \dot{u} Y_{l_j, \tau_j}) \} \quad (15)$$

Here $C_\alpha = (4\pi)^2 R_\alpha^4 / V$, index τ refers to m or (m, c) , (m, s) (in case of cos- and sin-like real spherical harmonics [41]) and the integrals are given be

$$(u Y_{l_1, \tau_1} | \vec{\nabla} u Y_{l_2, \tau_2}) = \int_0^{R_{MT}^\alpha} \int_\Omega u_{l_1}(r) Y_{l_1, \tau_1}^*(\Omega) \vec{\nabla} \{ u_{l_2}(r) Y_{l_2, \tau_2}(\Omega) \} r^2 dr d\Omega. \quad (16)$$

Although in Eq. (15) in principle we deal with a double sum, Eq. (16) acts as a selection rule and greatly reduces the number of non-zero terms in Eq. (15). In fact, the non-zero terms are only those for which

$$l_t = l_j \pm 1,$$

which is imposed by the parity consideration.

Explicit expressions for the integrals $(uY_{l_1, \tau_1}|\vec{\nabla}uY_{l_2, \tau_2})$ can be worked out with the help of equations in Sec. 5.8.3 of Ref. [47] (see also Appendix A of [30]), noting that $\partial_x = (-\nabla_{+1} + \nabla_{-1})/\sqrt{2}$, $\partial_y = i(\nabla_{+1} + \nabla_{-1})/\sqrt{2}$ and $\partial_z = \nabla_0$. Since the operator of momentum is hermitian, Eq. (15) should be symmetrized in respect to $\vec{\nabla}$ operating on the functions standing on the right and left sides of Eq. (15). (The same result is obtained by taking into full account the integration on the surface region of MT-sphere.)

It is worth considering these equations for a system having the inversion symmetry, for example, for the diamond, Fig. 1. In that case there are two equivalent MT-spheres, and the expression $\exp(i\vec{K}_{tj}\vec{R}_\alpha)$ in Eq. (12b) and Eq. (14) should be replaced by the sum over two MT-spheres (i.e. $\alpha = 1, 2$) with $\vec{R}_{\alpha=1,2} = \pm\vec{R}_1$, where $\vec{R}_1 = (1, 1, 1)a_{latt}/8$. In Eq. (12b) the summation gives the standard LAPW structure factor $\sum_{\alpha=1}^2 \exp(i\vec{K}_{tj}\vec{R}_\alpha) = 2\cos(\vec{K}_{tj}\vec{R}_1)$. Thus, the matrix elements of L_H^I , Eqs. (12a)–(12c), and consequently M_H^I , are imaginary. The same consideration, applied to the term in square brackets of Eq. (14), yields $[\vec{n}_H \times \vec{\mathcal{R}}]$, where

$$\vec{\mathcal{R}} = \sum_{\alpha=1}^2 \vec{R}_\alpha e^{i\vec{K}_{tj}} = 2i\vec{R}_1 \sin(\vec{K}_{tj}\vec{R}_1). \quad (17)$$

Since in terms of real spherical harmonics $\langle \vec{P}(\vec{k}, \alpha) \rangle$, Eq. (15), is real, the matrix elements of $L_H^{MT,II}$, Eq. (14), and $M_H^{MT,II}$ are imaginary. Consequently, the matrix elements of L_H^{MT} , Eq. (13), and the full magnetic moment $M_H^{MT} = \mu_B L_H^{MT}$ inside the MT-spheres are also imaginary.

C. Van Vleck contribution from the interstitial region

Here we calculate the matrix elements of L_H^{IR} and M_H^{IR} for the interstitial region (IR). Starting with the plane wave expression for the LAPW basis functions, Eq. (10), and using $\vec{L} = -i[\vec{r} \times \vec{\nabla}]$ we obtain

$$\langle t | L_H^{IR}(\vec{k}) | j \rangle = \frac{1}{V} \int_{IR} e^{i\vec{K}_{tj}\vec{r}} [\vec{r} \times (\vec{k} + \vec{K}_j)] d\vec{r}, \quad (18)$$

where the integration is taken over the interstitial region. Taking into account the hermiticity of \vec{L} (or, equivalently, treating accurately the MT-sphere surface integration),

and adapting the situation to the unit cell inversion symmetry, Eq. (18) can be rewritten as

$$\langle t | L_H^{IR}(\vec{k}) | j \rangle = [\vec{n}_H \times \vec{\mathcal{I}}_{tj}] \left(\vec{k} + \frac{1}{2}(\vec{K}_t + \vec{K}_j) \right), \quad (19a)$$

where

$$\vec{\mathcal{I}}_{tj} = \frac{1}{V} \int_{IR} e^{i\vec{K}_{tj}\vec{r}} \vec{r} d\vec{r}. \quad (19b)$$

The integral $\vec{\mathcal{I}}_{tj}$, Eq. (19b), comprises three components $\mathcal{I}_{tj,x}$, $\mathcal{I}_{tj,y}$ and $\mathcal{I}_{tj,z}$, which can be found in analytical form from

$$\mathcal{I}_{tj,x} = -i \left(\frac{\partial}{\partial K_{tj,x}} O_{tj}^{IR} \right), \quad (20a)$$

and analogous relations for the y - and z -components. Here

$$O_{tj}^{IR} = \frac{1}{V} \int_{IR} e^{i\vec{K}_{tj}\vec{r}} d\vec{r} \quad (20b)$$

is the well known LAPW overlap integral in the interstitial region. It is worth mentioning that Eq. (20a) and Eq. (20b) should be treated with care – for example, cases with $O_{tj}^{IR} = 0$ can result in $\partial O_{tj}^{IR} / \partial K_{tj,x} \neq 0$. More details on analytic expressions for $\vec{\mathcal{I}}_{tj}$ are given in Appendix B.

Finally, we note that for diamond and other cases with inversion symmetry, the overlap integrals O_{tj}^{IR} are real while the components of $\vec{\mathcal{I}}_{tj}$ are imaginary, leading to imaginary matrix elements for L_H^{IR} and M_H^{IR} , Eq. (18).

IV. METHOD: LANGEVIN DIAMAGNETISM

In contrast to the Van Vleck paramagnetism operating with wave functions of states and their energies, the evaluation of the Langevin (Larmor) diamagnetism is based only on the knowledge of the electron densities ($\rho_{val}(\vec{r})$ and $\rho_c(\vec{r})$ of the valence and core electrons, respectively) and the direction \vec{n}_H of the applied magnetic field H . As discussed in Sec. II, in calculating the diamagnetic response from the interstitial region we should use direct equations (1), (3) with perpendicular component of radius-vector r_\perp , counted from $\vec{R}_0 = 0$.

The same holds for the calculation of the MT-sphere contribution $\langle r_\perp^2 \rangle_{val}^{MT}$ from the valence electrons. However, from the technical point of view it is more convenient to compute first the quantity $\chi_{MT,0}^{dia} = -C_L \langle (\vec{r} - \vec{R}_c)_\perp^2 \rangle_{val}^{MT}$ with r_\perp , counted from the MT-sphere center \vec{R}_c . In that case, as follows from Eq. (4), in addition to $\chi_{MT,0}^{dia}$ the diamagnetic response χ_{MT}^{dia} acquires also the extra (offset) contribution $\chi_{MT,off}^{dia} = -C_L R_{c,\perp}^2 |Q_{val}^{MT}|$. (We recall that $R_{c,\perp}$ is the perpendicular component of \vec{R}_c , and Q_{val}^{MT} is the total charge of the valence electrons inside the sphere.)

In the following we apply our method to diamond. Taking into account that there are two MT-spheres in the unit cell, for the MT valence contribution we obtain

$$\chi_{MT,v}^{dia} = 2\chi_{MT,0,v}^{dia} + \chi_{MT,off,v}^{dia}, \quad (21a)$$

where the offset term is given by

$$\chi_{MT,off,v}^{dia} = -2C_L R_{c,\perp}^2 |Q_{val}^{MT}|. \quad (21b)$$

Here $\chi_{MT,0,v}^{dia}$ is the diamagnetic contribution of the valence electrons from a single MT-sphere with r_{\perp} counted from the sphere center, which can be rewritten in the familiar form,

$$\chi_{MT,0,v}^{dia} = -\frac{2}{3}C_L \langle r^2 \rangle_{val}, \quad (22)$$

where $\langle r^2 \rangle_{val}$ is the value of r^2 for valence electrons averaged inside the sphere with the spherically symmetric component $\rho_{val}^{L=0}(r)$ of the valence density. For diamond the high multipole moments with $L > 2$ do not contribute to $\chi_{MT,0,v}^{dia}$. Indeed, $r_{\perp}^2 = c_0 Y_{L=0,0} + c_{\tau} Y_{L=2,\tau}$ and from symmetry it follows that the nonzero integral over r_{\perp}^2 can be only with density components with $L = 0, 2$, whereas in diamond the first non-zero density multipole is an octupole with $L = 3$ [41].

In principle, Eq. (21a) should also be employed for the diamagnetic response $\chi_{MT,c}$ from the core electrons. However, as discussed in the end of Sec. II, the core contribution can be calculated more easily choosing the gauge origin, coinciding with the MT-sphere center. For core diamagnetic part we then obtain $\chi_c^{dia} = \chi_{MT,0,c}^{dia}$, with the paramagnetic counterpart $\chi_c^{para} = 0$, because the orbital magnetic moment for the 1s core states is zero. The total magnetic response from the core electrons is

$$\chi_{MT,c} = 2\chi_{MT,0,c}^{dia}, \quad (23)$$

where $\chi_{MT,0,c}^{dia}$ is given by Eq. (22) with $\langle r^2 \rangle_{val}$ substituted by $\langle r^2 \rangle_c$.

V. DIAMAGNETISM AND ANISOTROPY OF χ IN DIAMOND

Here we consider the magnetic susceptibility of pristine diamond applying the formulas from Sec. III. and Sec. IV to the calculation of χ^{dia} , χ^{para} and χ^{tot} .

One of the most important consequences of the induced magnetization, caused by the external magnetic field H is the emergence of a new crystalline symmetry, which takes into account the direction \vec{n}_H of \vec{H} . For example, if \vec{n}_H is collinear to the [111] axis, the initial cubic symmetry is reduced to the three-fold rotation symmetry C_{3v} about [111]. If \vec{n}_H is parallel to the [001] axis, the new symmetry is the four-fold rotation C_{4v} about [001], etc. For the general direction of \vec{n}_H ($n_{H,x} < n_{H,y} < n_{H,z}$) there is no crystal point symmetry and the only remaining symmetry operation is inversion. In our calculations we have observed these effects explicitly.

TABLE I. Contributions χ^L to the Langevin diamagnetic response χ^{dia} (tot.) for various directions of \vec{H} from the valence electrons (val.), interstitial region (IR), and the offset term, Eq. (21b), LDA calculations with a_{latt}^{exp} ; all χ are volume values, in units 10^{-7} , see text for details.

$\vec{H} \parallel$	χ^L , val.	χ^L , IR	χ^L , offset	χ^{dia} , tot.
[1, 1, 1]	-18.146	-11.452	0	-18.614
[1, 1, -1]	-46.207	-39.513	-16.356	-46.675
[0, 0, 1]	-39.192	-32.498	-12.267	-39.659
[1, -1, 0]	-49.714	-43.020	-18.400	-50.182
[-a ₁ , a ₁ , b ₁]	-44.048	-37.354	-15.097	-44.516
[a ₂ , b ₂ , 0]	-32.798	-26.104	-8.540	-33.265

A. Langevin diamagnetic contributions

First, we consider the Langevin diamagnetic response χ^{dia} , which has two main contributions – from the valence and core electrons, $\chi^{dia}(\text{tot.}) = \chi^L(\text{val.}) + \chi^L(\text{core})$. The core contribution is given by the MT value $\chi^L(\text{core}) = \chi_{MT,c}$, Eq. (23), our LDA calculation yields $-0.468 \cdot 10^{-7}$ [24] for all \vec{n}_H . In turn, the valence contribution consists of two parts, $\chi^L(\text{val.}) = \chi^L(\text{IR}) + \chi^L(\text{MT})$, from the interstitial region (IR) and MT-spheres (MT). The latter, Eq. (21a), includes also the offset term $\chi^L(\text{offset})$, Eq. (21b). In the interstitial region the value of r_{\perp}^2 is directly determined by \vec{n}_H , which explicitly changes the integral $\langle r_{\perp}^2 \rangle$, Eq. (3). The dependence of some contributions on \vec{n}_H is demonstrated in Table I. (The directions $[-a_1, a_1, b_1]$ and $[a_2, b_2, 0]$ in Table I, belong to the 74 point Lebedev grid [48, 49], used for a precise surface integration; $a_1 = 0.480384$, $b_1 = 0.733799$, and $a_2 = 0.320773$, $b_2 = 0.947156$). The \vec{n}_H -independent MT valence contribution, determined by Eq. (22), is $-6.694 \cdot 10^{-7}$ (LDA). Thus, the dependence of $\chi_{MT,v}^{dia}$ on \vec{n}_H is solely due to the offset term $\chi_{MT,off,v}^{dia}$, Eq. (21b), which explicitly depends on $R_{c,\perp}$.

It is worth mentioning that after fixing \vec{n}_H the calculation of all Langevin contributions requires only the valence (ρ_{val}) and core (ρ_c) electron density, taken from band structure calculations. Both ρ_{val} and ρ_c are obtained using the standard irreducible part of the Brillouin zone. For diamond the irreducible part, shown in Fig. 2a, is only 1/48 part of the whole Brillouin zone. Thus, the diamagnetic Langevin contribution χ^{dia} can be obtained using the band structure calculations with the standard (1/48) irreducible part of the Brillouin zone. The situation is very different for the Van Vleck paramagnetic response χ^{para} considered below.

B. Enhanced irreducible part of the Brillouin zone in calculations of Van Vleck contributions

To deal with various k -point contributions to χ^{para} , Eq. (7), we will partition the total k -sum in Eq. (7) in subsums, each of which is limited to a certain part of

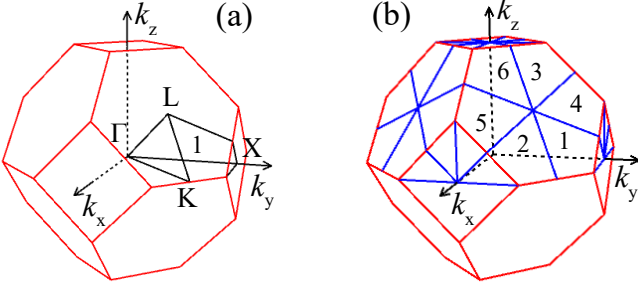


FIG. 2. The Brillouin zone of the diamond structure in reciprocal (k) space. (a) Irreducible part of BZ (1/48) without external magnetic field; (b) Irreducible part of BZ (upper half, 1/2) in the presence of magnetic field, divided into 24 subsections, each of which is equivalent to the part 1 shown in (a).

the Brillouin zone, shown schematically in Fig. 2b. We will classify these parts as follows. The first six parts, having the same volume ($V_k/48$) in k -space, are shown in Fig. 2b explicitly. The other 18 parts are obtained from these six ones by rotations by angles $\pi/2$, π , $3\pi/2$ about the [001] four-fold rotation axis. Correspondingly, we will denote them as \mathcal{N}_r , where $n = 1, 2, \dots, 6$ refers to the parts shown in Fig. 2b, and $r = 0, 1, 2, 3$ refers to the subsequent rotation about the [0,0,1]-axis by the angle $\varphi = 0, \pi/2, \pi, 3\pi/2$. These 24 subregions of \mathcal{N}_r make up the upper half of the entire Brillouin zone, and given that the inversion symmetry is preserved in an applied magnetic field, this is sufficient for a complete description. Our study shows that indeed for the calculations of the Van Vleck contribution along some directions of H , summations over all 24 subparts \mathcal{N}_r are required, details are given in Appendix C. Thus, the irreducible part of the Brillouin zone for diamond in an external magnetic field includes the entire upper half of the zone, shown in Fig. 2b.

C. Analyses of χ^{tot} for various directions of magnetic field

In this subsection we analyze the resulting total magnetic susceptibility $\chi^{tot}(\vec{n}_H) = \chi^{dia}(\vec{n}_H) + \chi^{para}(\vec{n}_H)$ for various directions \vec{n}_H of magnetic field H . The results for some selected values of \vec{n}_H are reproduced in Table II. A comparative study of partial contributions to χ^{para} from the interstitial region and MT-sphere region is given in Appendix D.

We first discuss the case of \vec{H} parallel to the z -axis, $\vec{n}_H = (0, 0, 1)$. The same contributions χ^{tot} , χ^{dia} and χ^{para} occur for \vec{H} parallel to the x -axis and y -axis. This is a consequence of the symmetry of the chosen unit cell, Fig. 1, and the Brillouin zone, Fig. 2. Indeed, the subsequent counterclockwise rotations by $2\pi/3$ about the [1,1,1]-axis transform the unit cell and Brillouin zone into themselves, whereas the z -axis transforms to the x -axis

TABLE II. Full diamagnetic (Langevin) response χ^{dia} , and full paramagnetic (Van Vleck) response χ^{para} , and their sum χ^{tot} for selected directions \vec{n}_H of \vec{H} . The subscript av of \vec{n}_H stands for χ^{dia} , χ^{para} , χ^{tot} averaged over all equivalent directions \vec{n}'_H , see text for details. LDA calculations with a_{latt}^{LDA} , all χ are volume values, in units 10^{-7} .

$\vec{H} \parallel$	χ , LDA			χ , GGA		
	dia	para	tot	dia	para	tot
[0, 0, 1]	-39.662	23.136	-16.526	-39.598	23.054	-16.544
[0, 0, 1] _{av}	-39.662	23.136	-16.526	-39.598	23.054	-16.544
[1, 1, 1]	-18.616	10.712	-7.904	-18.592	10.662	-7.930
[1, 1, -1]	-46.678	27.276	-19.402	-46.600	27.185	-19.415
[1, 1, 1] _{av}	-39.662	23.136	-16.526	-39.598	23.054	-16.544
[1, 1, 0]	-29.139	16.924	-12.215	-29.095	16.858	-12.237
[1, -1, 0]	-50.186	29.348	-20.838	-50.101	29.250	-20.851
[1, 1, 0] _{av}	-39.662	23.136	-16.526	-39.598	23.054	-16.544
[a ₁ , a ₁ , b ₁]	-19.968	11.510	-8.458	-19.941	11.458	-8.483
[-a ₁ , a ₁ , b ₁]	-44.519	26.003	-18.516	-44.445	25.914	-18.531
[-a ₁ , -a ₁ , b ₁]	-49.643	29.028	-20.615	-49.560	28.931	-20.629
[a ₁ , a ₁ , b ₁] _{av}	-39.662	23.136	-16.526	-39.598	23.054	-16.544
[a ₂ , b ₂ , 0]	-33.268	19.361	-13.907	-33.216	19.289	-13.927
[-a ₂ , b ₂ , 0]	-46.056	26.910	-19.146	-45.980	26.819	-19.161
[a ₂ , b ₂ , 0] _{av}	-39.662	23.136	-16.526	-39.598	23.054	-16.544

and then to the y -axis.

However, if we consider H applied along main cube diagonals (i.e. [1,1,1], [1,1,-1], [-1,1,1] and [1,-1,1]), the situation is different. In that case, $\chi^{tot}(\vec{n}_H)$, $\chi^{dia}(\vec{n}_H)$ and $\chi^{para}(\vec{n}_H)$, found for these directions, are not equal. In Table II we quote these values for [1,1,1] and [1,1,-1]. Note, that the rotation about the [1,1,1]-axis transforms the [1,1,-1]-axis first to [-1,1,1], and then to [1,-1,1]. Thus, the values of $\chi^{tot}(\vec{n}_H)$, $\chi^{dia}(\vec{n}_H)$ and $\chi^{para}(\vec{n}_H)$ should be the same for [1,1,-1], [-1,1,1] and [1,-1,1], which was confirmed by our direct calculations. Since in real diamond crystal these directions are equivalent, we consider the average value of χ^{tot}_{av} , χ^{dia}_{av} and χ^{para}_{av} , calculated according to the occurrence of individual values, i.e.

$$\chi[1, 1, 1]_{av} = (\chi[1, 1, 1] + 3\chi[1, 1, -1])/4. \quad (24)$$

This average value is given in Table II as [1, 1, 1]_{av}. Note, that it exactly corresponds to [0, 0, 1]_{av} (i.e. when H is parallel to [0,0,1], [1,0,0] or [0,1,0]). In fact, as follows from Table II, the average values χ^{tot}_{av} , χ^{dia}_{av} and χ^{para}_{av} are the same for any direction \vec{n}_H of the magnetic field: they represent the actual magnetic susceptibility and its full diamagnetic and paramagnetic contribution.

In Table II this conclusion has been checked for six equivalent directions [1, 1, 0], [1, -1, 0], etc. with two non-equivalent χ -values, for 12 equivalent directions [a₁, a₁, b₁], [a₁, b₁, a₁] etc. with three non-equivalent χ -values, and for 12 equivalent directions [a₂, b₂, 0], [a₂, 0, b₂] etc. with two non-equivalent χ -values. Here two groups of \vec{n}_H -directions – [a₁, a₁, b₁] and [a₂, b₂, 0] – belong to the 74 point Lebedev grid [48, 49], used for accurate surface integration, where $a_1 \approx 0.480384$,

$$b_1 = \sqrt{1 - 2a_1^2}, \text{ and } a_2 \approx 0.320773, b_2 = \sqrt{1 - a_2^2}.$$

The procedure of averaging used in this subsection, can be viewed as an analogue of the symmetrization of the electron density obtained at a \vec{k} -point in accordance with its full crystal symmetry.

D. Invariance of χ^{tot} , χ^{dia} and χ^{para} in respect to the direction of magnetic field

If the magnetic susceptibility $\chi^{tot}(\vec{n}_H)$ is anisotropic in respect to the direction \vec{n}_H of magnetic field, defined by the polar angles $\vec{n}_H \equiv (\theta, \varphi)$, it can be expanded in multipolar series,

$$\chi^{tot}(\theta, \varphi) = \chi_0 + \chi_4 K_{L=4}(\theta, \varphi) + \chi_6 K_{L=6}(\theta, \varphi), \quad (25)$$

where χ_0 is the isotropic part, while the anisotropy is described by the cubic harmonics $K_{L=4}$, $K_{L=6}$, which are symmetry adapted combinations of spherical harmonics with $L = 4$ and 6, which are invariant under symmetry operations of the tetrahedral (T_d) point symmetry. The explicit form of $K_{L=4}$, $K_{L=6}$ can be found e.g. in [41]), and in Eq. (25) we have ignored the high multipole terms with $L \geq 8$. The coefficients χ_4 and χ_6 are found from

$$\begin{aligned} \chi_L &= \int_{\Omega} d\Omega \chi^{tot}(\theta, \varphi) K_L(\theta, \varphi) \\ &\rightarrow \sum_i w_i \chi^{tot}(\theta_i, \varphi_i) K_L(\theta_i, \varphi_i), \end{aligned} \quad (26)$$

where the integration on $\Omega = (\theta, \varphi)$ is replaced by summation on points (θ_i, φ_i) with the weight w_i . To perform the summation in Eq. (26), we have used the 74 point Lebedev surface grid [48, 49], which is enough to extract the coefficients $\chi_{L=4}$ and $\chi_{L=6}$. Using results listed in Table II, we find that $\chi_4 = \chi_6 = 0$, and the only nonzero term in Eq. (25) is χ_0 . The same result holds for χ^{dia} and χ^{para} . Therefore, all magnetic susceptibilities (χ^{tot} , χ^{dia} and χ^{para}) are independent of the direction \vec{n}_H of the magnetic field H . The actual values of χ^{tot} , χ^{dia} and χ^{para} , obtained within the LDA and GGA variants of DFT, are collected in Table III.

In fact, the independence from \vec{n}_H is already present in Table II, manifesting itself in equal averaged values of χ_{av} . The integration, Eq. (26), ascertains that these averaged values are equal to the actual ones, Table III (the LDA variant at a_{latt}^{exp}).

The question may arise: why χ^{tot} , χ^{dia} and χ^{para} are different for some individual directions of \vec{H} , for example, for $[1, 1, 1]$ and $[1, 1, -1]$, Table II, although these crystal axes should be equivalent? We think that this is directly connected with the choice of the primitive unit cell. If we consider the primitive unit cell, chosen by us, Fig. 1, we find that its shape is not invariant under all symmetry operations of the diamond crystal lattice. This does not matter for electron band structure calculations because we impose the symmetry restrictions on the electron density by expanding it only in symmetry adapted

TABLE III. DFT results for χ^{dia} , χ^{para} , χ^{tot} (volume values, in 10^{-7}) for different lattice constants a_{latt} : (1) equilibrium LDA lattice constant a_{latt}^{LDA} ; (2) equilibrium GGA lattice constant a_{latt}^{GGA} ; (3) experimental lattice constant a_{latt}^{exp} . (*) and (**) experimental volume susceptibilities χ^{exp} , obtained from (*) density value $\chi_{\rho}^{exp} = -4.5 \times 10^{-7} \text{ cm}^3/\text{g}$ [20]; (**) molar value $\chi_m^{exp} = -5.9 \times 10^{-6} \text{ cm}^3/\text{mole}$ [19]. (a) equilibrium a_{latt} in Ref. [25].

type DFT	a_{latt}	χ^{dia}	χ^{para}	χ^{tot}
LDA	$3.549^{(1)} \text{ \AA}$	-39.940	23.219	-16.721
GGA	$3.592^{(2)} \text{ \AA}$	-39.216	22.942	-16.274
LDA	$3.567^{(3)} \text{ \AA}$	-39.662	23.136	-16.526
GGA	$3.567^{(3)} \text{ \AA}$	-39.598	23.054	-16.544
LDA [25]	3.52^a \AA			-16.35
LDA [25]	$3.57^{(3)} \text{ \AA}$			-16.44
exp.* [20]				-15.82
exp.** [19]				-17.27

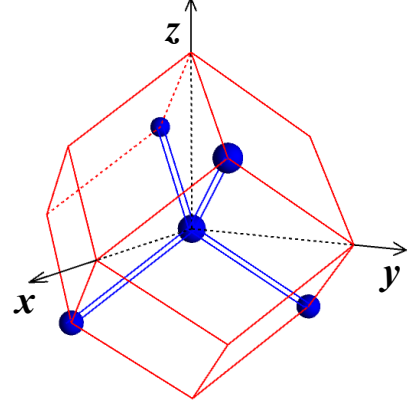


FIG. 3. The fully symmetrical (tetrahedral) diamond unit cell as a Wigner-Seitz primitive unit cell. One carbon atom is at the center (with weight $w = 1$), the four remaining atoms lie at vertices ($w = 1/4$); together they represent the two carbon atoms in the unit cell (compare with Fig. 1). The double blue lines represent C-C carbon bonds.

functions inside the MT-spheres and in stars of \vec{K}_j in the interstitial region [37]. In the magnetic calculation, the symmetry restrictions are equivalent to the introduced procedure of averaging, e.g. in Eq. (24). The equivalence of the individual directions $[1, 1, 1]$ and $[1, -1, 1]$ and all others, can be explicitly restored if one uses the primitive unit cell, reproduced in Fig. 3. This is the Wigner-Seitz unit cell having the full tetrahedral site symmetry. Although this choice of unit cell looks very attractive, it removes the inversion and requires working with partial occupancy of four carbon atoms, which is inconvenient in practical calculations.

VI. CONCLUSIONS

We have presented a general method for the calculation of all contributions to the Van Vleck paramagnetism and the Langevin diamagnetism and applied it to the calculation of the magnetic susceptibility χ^{tot} of diamond, which is a very important technological material. In contrast to other approaches [25–28, 30, 31], based on the initial linear response formulation of Mauri et al. [25, 27], the method (1) uses a single choice of the gauge for valence electrons throughout the whole crystal, and (2) works in the static external magnetic field H , i.e. no modulation with a small wave vector q of H is assumed, $q = 0$. The consideration is based on the statement (Appendix A) that the sum of the Van Vleck term, χ^{para} , and the Langevin term, χ^{dia} , constituting the total susceptibility $\chi^{tot} = \chi^{para} + \chi^{dia}$, is independent of the choice of the magnetic gauge origin, although individually χ^{para} and χ^{dia} can demonstrate such dependence.

The method is adapted for the LAPW basis functions, which are plane waves in the interstitial region, and atomic-like wave functions in the MT-sphere region, Eq. (10). Since we use a single choice of magnetic gauge for the whole crystal, we obtain unfamiliar contributions which we call offset terms. For example, such a term is given by the magnetic moment $M_H^{MT,II}$, Eq. (14), appearing when the MT-sphere center is displaced from the gauge origin. Likewise, the offset term is present in the Langevin calculation of χ^{dia} , Eq. (21b). Finally, we mention a contribution from the interstitial region, Sec. III C. All magnetic contributions are obtained in analytical form and then implemented in our LAPW code [39]. The method can be applied to any solid including dielectrics and metals. In metals it can be used for obtaining the Langevin contribution χ^{dia} and the Van Vleck contribution χ^{para} in addition to the well known Pauli paramagnetism and the Landau diamagnetism.

Applying this method to diamond, we have performed FLAPW calculations of χ^{para} , χ^{dia} and χ^{tot} , analyzing various partial contributions for different directions of the applied magnetic field H . We have found that the application of the magnetic field changes the crystal symmetry, which manifests itself in the enhanced irreducible part of the Brillouin zone, required for such calculations, Sec. V B and Fig. 2.

In study of diamond our goal was to extract the anisotropic part, described by the cubic harmonics $K_{L=4}(\vec{n}_H)$, $K_{L=6}(\vec{n}_H)$ in χ^{tot} , Eq. (25). For that purpose we have performed integration in Eq. (26), using the 74 point Lebedev surface grid [48, 49], and found that the anisotropic coefficients χ_4 , χ_6 in Eq. (25), are reduced to zero, i.e. $\chi_4 = \chi_6 = 0$. Note, however, that the calculated individual susceptibilities χ^{para} , χ^{dia} and χ^{tot} depend on the direction of H . We consider that as an artefact of the calculations, related to a relatively low symmetry of the chosen primitive unit cell, Fig. 1. In Sec. V D we argue that the individual susceptibilities χ^{para} , χ^{dia} will be independent of \vec{n}_H for the fully symmetric

Wigner-Seitz primitive unit cell of diamond, Fig. 3.

Thus, our calculations result in magnetic susceptibilities χ^{para} , χ^{dia} and χ^{tot} , quoted in Table III, which are independent of the direction \vec{n}_H of the applied magnetic field H . The calculated values χ^{tot} in other units lie in the range $-4.68\text{--}4.73 \times 10^{-7} \text{ cm}^3/\text{g}$ (mass magnetic susceptibility) and $-5.63\text{--}5.68 \times 10^{-6} \text{ cm}^3/\text{mole}$ (molar magnetic susceptibility). They are in very good correspondence with the experimental values: $-5.9 \times 10^{-6} \text{ cm}^3/\text{mole}$ [19] and $-4.5 \times 10^{-7} \text{ cm}^3/\text{g}$ [20], and previous LDA calculations of Mauri and Louie [25].

ACKNOWLEDGMENTS

This work was supported by the National Natural Science Foundation of China (Grant No. 12274102) and the Fundamental Research Funds for the Central Universities (Grant No. FRFCU5710053421, No. HIT.OCEF.2023031).

Appendix A

Here we prove that the sum $\chi^{tot} = \chi^{dia} + \chi^{para}$ of the Langevin (Larmor) diamagnetic response χ^{dia} and the Van Vleck paramagnetic response χ^{para} does not depend on the choice of the gauge origin [i.e. \vec{R}_0 in Eq. (2)], [32]. The change of the vector potential \vec{A} associated with \vec{R}_0 is in fact the degree of freedom, directly related to the choice of the gauge. The gauge transformation for \vec{A} can be written in the general form $\vec{A} \rightarrow \vec{A} + \vec{\nabla}f$, where $f(\vec{r})$ is an arbitrary coordinate function. In our case, Eq. (2), the function f is given by $f = -\vec{R}_0 \times \vec{H} \cdot \vec{r}/2$. In Ref. 40 it is demonstrated that the gauge transformation does not alter essentially the solution, resulting in the following transformation of the wave function: $\Psi \rightarrow \Psi \exp(-ief(\vec{r})/\hbar c)$. In particular, the electron energy $E(H)$ does not depend on the choice of $f(\vec{r})$ for any value of the magnetic field H . This implies that the energy $E(H) = E_0 - \chi^{tot} H^2/2$, taken in the second order of H , is also the same for any $f(\vec{r})$ and χ^{tot} does not depend on \vec{R}_0 . Since $\chi^{tot} = \chi^{dia} + \chi^{para}$, we have proved that the sum of Eq. (1) and Eq. (5) is independent of \vec{R}_0 .

Appendix B

Here we consider the integrals $\mathcal{I}_{tj,\nu}$, where $\nu = x, y, z$, Eq. (19b), used in calculation of the matrix elements of the orbital momentum L_H^{IR} in the interstitial region, Eq. (19a). Below we find them by means of Eq. (20a). In the following we will condense notation using $K_\nu \equiv K_{tj,\nu}$, $\mathcal{I}_\nu \equiv \mathcal{I}_{tj,\nu}$ and limit ourselves to the case of interstitial region which has the inversion symmetry. Then, starting with the standard expression for the overlap integral O_{tj}

[37–39], we obtain

$$\mathcal{I}_\nu = \mathcal{I}_\nu^0 - i(\mathcal{I}_\nu^1 + \mathcal{I}_\nu^2 + \mathcal{I}_\nu^3), \quad (\text{B1})$$

where the \mathcal{I}_ν^0 is connected with the plane wave integration over the whole unit cell, whereas \mathcal{I}_ν^n ($n = 1, 2, 3$) represent contributions from the MT-spheres, subtracted from \mathcal{I}_ν^0 . Since the overlap over the unit cell is given by

$$O^0 = \frac{2}{\vec{b}_1 \vec{K}} \sin\left(\frac{\vec{b}_1 \vec{K}}{2}\right) \frac{2}{\vec{b}_2 \vec{K}} \sin\left(\frac{\vec{b}_2 \vec{K}}{2}\right) \frac{2}{\vec{b}_3 \vec{K}} \sin\left(\frac{\vec{b}_3 \vec{K}}{2}\right),$$

where $\vec{b}_1, \vec{b}_2, \vec{b}_3$ are the corresponding basis vectors [41], for $\mathcal{I}_\nu^0 \sim \partial O^0 / \partial K_\nu$, Eq. (20a), we have nonzero contributions only if (1) $\vec{b}_1 \vec{K} \neq 0, \vec{b}_2 \vec{K} = \vec{b}_3 \vec{K} = 0$; or (2) $\vec{b}_2 \vec{K} \neq 0, \vec{b}_1 \vec{K} = \vec{b}_3 \vec{K} = 0$; or (3) $\vec{b}_3 \vec{K} \neq 0, \vec{b}_1 \vec{K} = \vec{b}_2 \vec{K} = 0$. In the first case, for example, we obtain

$$\mathcal{I}_\nu^0 = -i \frac{\vec{b}_{1,\nu}}{\vec{b}_1 \vec{K}} (-1)^m, \quad (\text{B2})$$

where the integer $m = \vec{b}_1 \vec{K} / 2\pi$. Further, in Eq. (B1)

$$\begin{aligned} \mathcal{I}_\nu^1 &= - \sum_\alpha C(\alpha) F'_{K,\nu}(\alpha, \vec{K}) \frac{j_1(K R_{MT}^\alpha)}{K}, \\ \mathcal{I}_\nu^2 &= - \sum_\alpha C(\alpha) R_{MT}^\alpha F(\alpha, \vec{K}) \frac{j'_1(K R_{MT}^\alpha)}{K} \hat{K}_\nu, \\ \mathcal{I}_\nu^3 &= \sum_\alpha C(\alpha) F(\alpha, \vec{K}) \frac{j_1(K R_{MT}^\alpha)}{K^2} \hat{K}_\nu. \end{aligned} \quad (\text{B3})$$

Here $j_1(x)$ is the spherical Bessel function ($l = 1$), $C(\alpha) = 4\pi(R_{MT}^\alpha)^2/V$, $\hat{K}_\nu = K_\nu/K$, and

$$F(\alpha, \vec{K}) = \sum_\beta \cos(\vec{K} \vec{R}_{\beta(\alpha)}),$$

where the summation on $\beta(\alpha)$ implies the summation over the equivalent atoms β of the same atom type α centered at $\vec{R}_{\beta(\alpha)}$. Finally,

$$F'_{K,\nu}(\alpha, \vec{K}) = - \sum_\beta R_{\beta(\alpha),\nu} \sin(\vec{K} \vec{R}_{\beta(\alpha)}),$$

where $R_{\beta(\alpha),\nu}$ is the ν -th component of $\vec{R}_{\beta(\alpha)}$. The same function appears in the contribution to $L_H^{MT,II}$ from displaced MT-spheres, Eq. (17). One can show that in general $F'_{K,\nu}(\alpha, \vec{K}) = i \mathcal{R}_\nu$.

Note that all matrix elements for \mathcal{I}_ν are explicitly imaginary, Eqs. (B1)–(B3).

Appendix C

Here we consider non-equivalent parts \mathcal{N}_r required for the calculation of the Van Vleck summation for selected

TABLE IV. Partial contributions $\chi^{VV}(\mathcal{N}_r)$ to the Van Vleck paramagnetic response $\chi^{para} = 10.712$ for $\vec{H} \parallel [1, 1, 1]$ from various parts \mathcal{N}_r of BZ, LDA calculations with a_{latt}^{exp} ; χ – volume values, in 10^{-7} , $W_0 = 48$, N_{eq} is the number of equivalent parts in BZ, W is the total weight of $\chi^{VV}(\mathcal{N}_r) \cdot W_0$ in χ^{para} .

\mathcal{N}_r	$\chi^{VV}(\mathcal{N}_r) \cdot W_0$	N_{eq}	W
1_0	8.113	12	1/4
1_1	11.737	12	1/4
1_2	10.941	12	1/4
1_3	12.057	12	1/4

directions of H . Suppose we take \vec{H} parallel to the [1,1,1]-axis (i.e. $\vec{n}_H = (1, 1, 1)/\sqrt{3}$) and calculate contributions to χ^{para} , Eq. (7), from different subparts \mathcal{N}_r . In this particular case, both the Brillouin zone and the unit cell, Fig. 1, have common symmetry operations associated with the [1,1,1] three-fold rotation axis and some mirror planes (e.g. $x = y$). As a result, all subsums to χ^{para} from first six parts ($n_0, n = 1 - 6$) in Fig. 2 are equal. Among the remaining 18 parts ($\mathcal{N}_r, n = 1 - 6, r = 1, 2, 3$) there are three groups with 6 equal contributions. These findings are summarized in Table IV.

If however we consider \vec{H} parallel to the [1,1,-1]-axis (i.e. $\vec{n}_H = (1, 1, -1)/\sqrt{3}$) then there will be no common three-fold rotation symmetry shared both the Brillouin zone and the unit cell. In that case, in addition to inversion we have only the $x = y$ mirror plane, and the number of nonequivalent parts of the Brillouin zone is increased from four, quoted in Table IV, to twelve, which are $1_r, 3_r$ and 4_r ($r = 0, 1, 2, 3$). The same nonequivalent parts of the Brillouin zone are involved if \vec{H} is collinear to the [0,0,1]-axis, Table V, because in that case, as before, the only common point symmetry operation is the same $x = y$ mirror plane.

In general however, computation of all nonequivalent 24 contributions from the subparts of \mathcal{N}_r is necessary for χ^{para} . In particular, this is required if \vec{H} parallel to $[a, b, 0]$ and $[-a, a, b]$ ($a \neq b$).

Appendix D

Here we reproduce and compare partial contributions to χ^{para} for $\vec{H} \parallel [0, 0, 1]$. Earlier, we have analyzed the contributions $\chi^{VV}(\mathcal{N}_r)$ from nonequivalent parts \mathcal{N}_r of the Brillouin zone. Now we will consider contributions to $\chi^{VV}(\mathcal{N}_r)$ from various sources: the interstitial region, MT-sphere region, and from the offset term $M_H^{MT,II}$, Eq. (14). Our results are given in Table V.

It is worth noting that we obtain contributions from these sources to the total magnetic moment M_H in matrix form, Eq. (9), using LAPW basis functions ϕ_j , Eq. (10). At that level we have the property of additivity, i.e. $\langle t | M_H | j \rangle = \langle t | M_H^{IR} | j \rangle + \langle t | M_H^{MT} | j \rangle$. However, then we

TABLE V. Contributions $\chi' = \chi^{VV} \cdot W_0$ to the Van Vleck paramagnetic response $\chi^{para} = 23.136$ for $\vec{H} \parallel [0, 0, 1]$ from the interstitial region (IR), MT-sphere region (MT) and the offset part with $M_H^{MT,II}$, Eq. (14), for various parts \mathcal{N}_r of BZ, LDA calculations with a_{latt}^{exp} ; all χ are volume values, in units 10^{-7} , $W_0 = 48$; see text for details.

\mathcal{N}_r	χ', IR	χ', MT	χ', offset	χ', total
1 ₀	14.836	12.951	7.480	22.010
1 ₁	15.020	12.708	7.148	22.153
1 ₂	15.173	13.265	7.480	22.577
1 ₃	15.099	12.845	7.148	22.547
3 ₀	15.385	14.717	7.450	26.256
3 ₁	15.000	14.459	7.230	25.500
3 ₂	15.068	14.582	7.450	25.153
3 ₃	15.255	14.399	7.230	25.705
4 ₀	14.927	12.055	7.387	20.372
4 ₁	15.201	12.404	7.240	21.607
4 ₂	15.521	12.872	7.387	22.500
4 ₃	15.229	12.228	7.240	21.248

transform the matrices to the basis of band eigenstates, after which the magnetic moments are squared and substituted in Eq. (7). The last procedure obviously destroys the initial additivity. Therefore, in obtaining a particular

contribution in Table V the other terms were artificially put to zero. The MT contribution M_H^{MT} includes the offset contributions $M_H^{MT,II} = \mu_B L_H^{MT,II}$, Eq. (13), and Eq. (14). The column with the offset contributions in Table V was calculated when $M_H = M_H^{MT,II}$. Inspection of the data of Table V indicates that the contributions from the IR and MT regions are almost equal for all \mathcal{N}_r , with the IR contribution being somewhat larger. The offset contribution, on the other hand, is typically smaller – approximately 1/3 of the total value of χ^{VV} . Nevertheless, it accounts for more than half of the MT-contribution.

All partial contributions χ in Tables IV and V are enhanced by the factor $W_0 = 48$. Thus, they are scaled to the whole Brillouin zone as if all parts were equivalent to the chosen \mathcal{N}_r . In reality, for every row (\mathcal{N}_r) in Table V there are only four equivalent parts (N_{eq}) in BZ with the same value. Therefore, the weight of every part in Table V is $W = 1/12$, and to obtain the true contribution from the whole BZ one has to average the values in columns. That results in $\chi^{VV}(\text{IR})=15.143$ for the interstitial region, $\chi^{VV}(\text{MT})=13.290$ for the MT region, the offset value is $\chi^{VV}(\text{MT,II})=7.323$, and the total Van Vleck contributions is $\chi^{VV}=23.136$, in units of 10^{-7} (volume values).

[1] D. Awschalom, M. Flatté, Challenges for semiconductor spintronics. *Nature Phys.* **3**, 153 (2007).

[2] J. F. Barry, J. M. Schloss, E. Bauch, M. J. Turner, C. A. Hart, L. M. Pham, et al. Sensitivity optimization for NV-diamond magnetometry. *Rev. Mod. Phys.* **92**, 015004 (2020).

[3] N. Nunn, M. D. Torelli, A. Ajoy, A. I. Smirnov, and O. Shenderova, Beauty beyond the Eye: Color Centers in Diamond Particles for Imaging and Quantum Sensing Applications, *Reviews and Advances in Chemistry*, **12**, 1 (2022).

[4] J.P. King, K. Jeong, C.C. Vassiliou, C.S. Shin, R.H. Page, C.E. Avalos, H-J. Wang, A. Pines, Room-temperature in situ nuclear spin hyperpolarization from optically pumped nitrogen vacancy centres in diamond, *Nat. Commun.* **6**, 8965 (2015).

[5] J.P. King, P.J. Coles, J.A. Reimer, Optical polarization of ^{13}C nuclei in diamond through nitrogen vacancy centers, *Phys. Rev. B* **81**, 073201 (2010).

[6] J. Henshaw, D. Pagliero, P. R. Zangara, M. B. Franzoni, A. Ajoy, R. H. Acosta, J. A. Reimer, A. Pines, and C. A. Meriles, Carbon-13 dynamic nuclear polarization in diamond via a microwave-free integrated cross effect, *Proc. Natl. Acad. Sci. USA* **116**, 18334 (2019).

[7] C. Müller, X. Kong, J.-M. Cai, K. Melentijević, A. Stacey, M. Markham, et al. Nuclear magnetic resonance spectroscopy with single spin sensitivity. *Nat. Commun.* **5**, 4703 (2014).

[8] G. Balasubramanian, et al. Nanoscale imaging magnetometry with diamond spins under ambient conditions. *Nature* **455**, 648 (2008).

[9] J. R. Maze, et al. Nanoscale magnetic sensing with an individual electronic spin in diamond. *Nature* **455**, 644–647 (2008).

[10] N. Zhao, J.-L. Hu, S.-W. Ho, J. T. K. Wan, and R.-B. Liu, Atomic-scale magnetometry of distant nuclear spin clusters via nitrogen-vacancy spin in diamond. *Nat. Nanotech.* **6**, 242 (2011).

[11] L. P. McGuinness, et al. Quantum measurement and orientation tracking of fluorescent nanodiamonds inside living cells. *Nat. Nanotechnol.* **6**, 358 (2011).

[12] B. B. Buckley, G. D. Fuchs, L. C. Bassett, and D. D. Awschalom, Spin-light coherence for single-spin measurement and control in diamond. *Science* **330**, 1212 (2010).

[13] S. Pezzagna, and J. Meijer, Quantum computer based on color centers in diamond. *Appl. Phys. Rev.* **8**, 011308 (2021).

[14] G. Stevanato, J. T. Hill-Cousin, P. Håkansson, S. S. Roy, L. J. Brown, R. C. Brown, et al. A nuclear singlet lifetime of more than one hour in room-temperature solution. *Angew. Chem. Int. Ed.* **54**, 3740 (2015).

[15] F. Shagieva, S. Zaiser, P. Neumann, D.B.R. Dasari, R. Stöhr, A. Denisenko, R. Reuter, C.A. Meriles, J. Wrachtrup, Microwave assisted cross-polarization of nuclear spin ensembles from optically pumped nitrogen-vacancy centers in diamond, *Nano Lett.* **18**, 3731 (2018).

[16] B.L. Green, B.G. Breeze, G.J. Rees, J.V. Hanna, J.-P. Chou, V. Ivády, A. Gali, M.E. Newton, All-optical hyperpolarization of electron and nuclear spins in diamond, *Phys. Rev. B* **96**, 054101 (2017).

[17] D. Pagliero, K.R. Koteswara Rao, P.R. Zangara, S. Dhomkar, H.H. Wong, A. Abril, N. Aslam, A. Parker, J. King, C.E. Avalos, A. Ajoy, J. Wrachtrup, A. Pines, C.A. Meriles, Multispin-assisted optical pumping of bulk

¹³C nuclear spin polarization in diamond, Phys. Rev. B **97**, 024422 (2018).

[18] A. P. Nizovtsev, S.Ya. Kilin, A. L. Pushkarchuk, V. A. Pushkarchuk, S. A. Kuten, H. Zhikol, et al. Non-flipping ¹³C spins near an NV center in diamond: hyperfine and spatial characteristics by density functional theory simulation of the C510 [NV]H252 cluster. New J. Phys. **20**, 023022 (2018).

[19] S. Hudgens, M. Kastner, and H. Fritzsche, Diamagnetic Susceptibility of Tetrahedral Semiconductors, Phys. Rev. Lett. **33**, 1552 (1974).

[20] J. Heremans, C.H. Olk, and D.T. Morelli, Magnetic susceptibility of carbon structures, Phys. Rev. B **49**, 15122 (1994).

[21] A.V. Nikolaev and B. Verberck, Diamagnetism of Diamond and Graphite, in *Carbon based magnetism*, Ed. T. Makarova and F. Palacio, Elsevier (2006), p. 245.

[22] V. P. Sukhatme and P. A. Wolff, Chemical-Bond Approach to the Magnetic Susceptibility of Tetrahedral Semiconductors, Phys. Rev. Lett. **35**, 1369 (1975).

[23] D. J. Chadi, R. M. White, and W. A. Harrison, Theory of the Magnetic Susceptibility of Tetrahedral Semiconductors, Phys. Rev. Lett. **35**, 1372 (1975).

[24] A.V. Nikolaev, M.Ye. Zhuravlev, L.L. Tao, Ab initio based study of the diamagnetism of diamond, silicon and germanium, J. Magn. Magn. Mater. **588**, 171394 (2023).

[25] F. Mauri and S. G. Louie, Magnetic Susceptibility of Insulators from First Principles, Phys. Rev. Lett. **76**, 4246 (1996).

[26] T. Gregor, F. Mauri, and R. Car, A comparison of methods for the calculation of NMR chemical shifts, J. Phys. Chem. **111**, 1815 (1999).

[27] F. Mauri, B. G. Pfrommer, and S. G. Louie, Ab Initio Theory of NMR Chemical Shifts in Solids and Liquids, Phys. Rev. Lett. **77**, 5300 (1996).

[28] C. J. Pickard and F. Mauri, All-electron magnetic response with pseudopotentials: NMR chemical shifts, Phys. Rev. B **63**, 245101 (2001).

[29] J. R. Yates, C. J. Pickard, and F. Mauri, Calculation of NMR chemical shifts for extended systems using ultrasoft pseudopotentials, Phys. Rev. B **76**, 024401 (2007).

[30] R. Laskowski and P. Blaha, Calculations of NMR chemical shifts with APW-based methods, Phys. Rev. B **85**, 035132 (2012).

[31] R. Laskowski and P. Blaha, Calculating NMR chemical shifts using the augmented plane-wave method, Phys. Rev. B **89**, 014402 (2014).

[32] J. H. Van Vleck. *The Theory of Electric and Magnetic Susceptibilities* (Oxford University Press, London 1932), p. 276.

[33] N.W. Ashcroft, and N.D. Mermin, (1976) *Solid State Physics*. Brooks/Cole Cengage Learning (1976).

[34] L. D. Landau and E. M. Lifshitz, *Statistical Physics* (Pergamon, Bristol, 1995), Vol. 5.

[35] Ch. Kittel, *Introduction to solid state physics* – 8th ed. John Wiley & Sons (2005).

[36] A. V. Nikolaev, Landau diamagnetic response in metals as a Fermi surface effect, Phys. Rev. B, **98**, 224417 (2018).

[37] D.J. Singh, L. Nordström, *Planewaves, Pseudopotentials, and the LAPW Method*, 2nd ed. (Springer, New York, 2006).

[38] P. Blaha, K. Schwarz, G. Madsen, D. Kvasnicka and J. Luitz, J. Luitz, WIEN2K: *An Augmented Plane Wave plus Local Orbitals Program for Calculating Crystal Properties* (Vienna University of Technology, Austria, 2001).

[39] A. V. Nikolaev, D. Lamoen, and B. Partoens, Extension of the basis set of linearized augmented plane wave (LAPW) method by using supplemented tight binding basis functions, J. Chem. Phys. **145**, 014101 (2016).

[40] L. D. Landau and E. M. Lifshitz, *Quantum Mechanics - Non-relativistic theory* (Pergamon, Bristol, 1995), Vol. 3.

[41] C. J. Bradley and A. P. Cracknell, *The Mathematical Theory of Symmetry in Solids*, (Clarendon, Oxford, 1972).

[42] G. Lehmann and M. Taut, On the numerical calculation of the density of states and related properties, Phys. Status Solidi B **54**, 469 (1972).

[43] J. P. Perdew, K. Burke, and M. Ernzerhof, Generalized Gradient Approximation Made Simple, Phys. Rev. Lett. **77**, 3865 (1996).

[44] P. A. M. Dirac, Note on Exchange Phenomena in the Thomas Atom, Proc. Camb. Philos. Soc. **26**, 376 (1930).

[45] J. P. Perdew and Y. Wang, Accurate and simple analytic representation of the electron-gas correlation energy, Phys. Rev. B **45**, 13244 (1992).

[46] A. V. Nikolaev, I. T. Zuraeva, G. V. Ionova, Spin-polarization and spin-orbit interactions in the LAPW method: application in description of 3d metals, and B. V. Andreev, Fizika Tverdogo Tela **35**, 414 (1993). [translation: Phys. Solid State **35**, 213 (1993)].

[47] D. A. Varshalovich, A. N. Moskalev, and V. K. Khersonskii *Quantum Theory of Angular Momentum and its applications*, vol. 1, Moscow, Fizmatlit (2017).

[48] V. I. Lebedev, Values of the nodes and weights of ninth to seventeenth order gauss-markov quadrature formulae invariant under the octahedron group with inversion, USSR Computational Mathematics and Mathematical Physics, **15**, 44 (1975).

[49] V.I. Lebedev, and D.N. Laikov, A quadrature formula for the sphere of the 131st algebraic order of accuracy, Doklady Mathematics, **59**, 477, (1999).